Chinese J. Chem. Eng., **11** (5) 571 – 576 (2003)

Kinetics of Liquid-Phase Hydrogenation of Benzene in a Metal Hydride Slurry System Formed by $MlNi_5$ and Benzene*

DAI Shiyao(代世耀)[a], XU Guohua(徐国华)[a,], AN Yue(安越)[a], CHEN Changpin(陈长聘)[b], CHEN Lixin(陈立新)[b] and WANG Qidong(王启东)[b]**

[a] Department of Chemical Engineering, [b] Department of Materials Science, Zhejiang University, Hangzhou 310027, China

Abstract The kinetics of liquid-phase hydrogenation of benzene in misch metal nickel-five ($MlNi_5$) and benzene slurry system was studied by investigating the influences of the reaction temperature, pressure, alloy concentration and stirring speed on the mass transfer-reaction processes inside the slurry. The results show that the whole process is controlled by the reaction at the surface of the catalyst. The mass transfer resistance at gas-liquid interface and that from the bulk liquid phase to the surface of the catalyst particles are negligible. The apparent reaction rate is zero order for benzene concentration and first order for hydrogen concentration in the liquid phase. The kinetic model obtained fits the experimental data very well. The apparent activation energy of the hydrogen absorption reaction of $MlNi_5$-C_6H_6 slurry system is 42.16 kJ·mol^{-1}.

Keywords hydrogen storage slurry, hydrogen storage alloy, aromatics, hydrogen absorption

1 INTRODUCTION

The concept of the metal hydride slurry was first proposed in 1980's[1,2]. By suspending metal hydride particles in those "chemical-inert" solvents the deformation or rupture of the vessels can be easily avoided because of the elimination of the particle fragmentation and the heat transfer in gas-solid systems can also be improved. Inspired by this concept, a novel idea on slurry formed by hydrogen storage alloys and unsaturated aromatics (*e.g.* benzene, toluene and naphthalene) was put forward from our research group[3]. Although both the hydrogen storage alloys and the unsaturated aromatics can be used as the hydrogen storage media, the capacity of the former is generally much less than that of the latter.

Benzene is an important chemical widely used in industry, but its severe toxicity makes it deleterious to the enviornment and human health. Hydrogenation of benzene is regarded as a good method for the treatment of the waste benzene, since the products of hydrogenation, such as cyclohexane and cyclohexene, are important organic products and can be used to synthesize Nylon-6 and Nylon-66. In addition, cyclohexane is considered to be a highly-efficient and promising hydorgen carrier in hydrogen cell and hydorgen electric power generation due to its high hydrogen storage density [7.19% (by mass) and 56 kg H_2 per unit volume (m^3)]. The hydrogenation of the unsaturated aromatics is a typical reaction, catalyzed by many metal hydrides and hydrogen storage alloys[4]. In our novel slurry system, the hydrogen storage capacity can be freely adjusted by changing the ratio of the alloys and the organics, hence the hydrogenation or dehydrogenation reaction of the hydrocarbons may be conducted in a relatively moderate reaction condition. This was demonstrated feasible in the slurry system formed by lanthanum-rich misch metal nickel-five ($MlNi_5$) and benzene[5–7].

In this work, we systematically studied the kinetics of the liquid-phase hydrogenation of benzene in $MlNI_5$-C_6H_6 slurry system. The influences of the temperature, system pressure, alloy concentration and the stirring speed on hydrogen absorption rates of the slurries were investigated. The experimental results revealed that the whole process was controlled by the reaction on the catalyst surface, the mass-transfer resistance is negligible. The apparent reaction order is zero for benzene and first order for hydrogen in liquid phase.

2 THEORETICAL ANALYSIS AND MODEL DEVELOPMENT

2.1 Kinetic analysis of the slurry reactor

This section considers the liquid-phase hydrogenation reaction of benzene in a slurry reactor with catalyst particles suspending in the liquid phase. The hydrogen gas was first bubbled into the slurry, where it was absorbed by the surrounding liquid. The ab-

Received 2002-09-19, accepted 2003-06-06.

* Supported by the State Key Project of Basic Research of China (TG2000026406) and the National Natural Science Foundation of China (No. 50071053).

** To whom correspondence should be addressed.

sorbed hydrogen then diffused from the bulk liquid to the particle surfaces where the catalytic reaction took place (Fig. 1). When pure hydrogen is used as reactant, there is no mass-transfer resistance from bulk gas (in the bubble) to bubble-liquid interface where the phase equilibrium exists. The rise of the bubbles through the liquid, along with mechanical agitation, is usually sufficient to eliminate the mass-transfer resistance in the bulk liquid. By assuming a first-order irreversible catalytic reaction at the particle surface, the apparent reaction rate at steady state can be written as[8]

$$r_{\rm obs} = k_{\rm obs} \cdot c_{\rm e} \tag{1}$$

where $c_{\rm e}$ is the equilibrium concentration of the hydrogen on the liquid side at the gas-liquid interface, and $k_{\rm obs}$ the apparent reaction rate constant with

$$\frac{1}{k_{\rm obs}} = \frac{1}{k_{\rm L}a_{\rm g}} + \frac{1}{a_{\rm p}}\left(\frac{1}{k_{\rm c}} + \frac{1}{k_{\rm s}}\right) \tag{2}$$

where $k_{\rm L}$ is the gas-liquid mass transfer coefficient on the liquid side at the gas-liquid interface, $k_{\rm c}$ is the liquid-solid mass transfer coefficient, $k_{\rm s}$ is the reaction rate constant at the solid surface, $a_{\rm g}$ is the specific surface area of bubbles per unit liquid volume and $a_{\rm p}$ is the specific surface area of particles per unit liquid volume. For spherical particles

$$a_{\rm p} = 6m/\rho_{\rm p}d_{\rm p} \tag{3}$$

where m is the catalyst load per unit liquid volume, $\rho_{\rm p}$ the density of the solid particles and $d_{\rm p}$ the mean particle size. Combination of Eqs. (1), (2) and (3) yields

$$\frac{c_{\rm e}}{r_{\rm obs}} = \frac{1}{k_{\rm L}a_{\rm g}} + \frac{\rho_{\rm p}d_{\rm p}}{6m}\left(\frac{1}{k_{\rm c}} + \frac{1}{k_{\rm s}}\right) \tag{4}$$

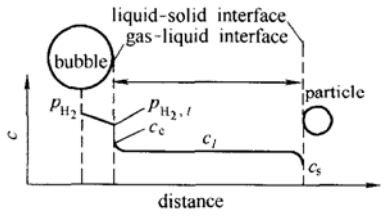

Figure 1 Schematic diagram of concentration distribution in the slurry

In terms of Eq. (4), $\frac{\rho_{\rm p}d_{\rm p}}{6m}\frac{1}{k_{\rm c}}$ reflects the mass transfer resistance of hydrogen from bulk liquid to the surface of the catalyst particles, $\frac{\rho_{\rm p}d_{\rm p}}{6m}\frac{1}{k_{\rm s}}$ the reaction resistance at the surface of the catalyst particles, and $\frac{1}{k_{\rm L}a_{\rm g}}$ the mass transfer resistance on the liquid side at gas-liquid interface. Eq. (4) indicates that a plot of $c_{\rm e}/r_{\rm obs}$ *vs.* $1/m$ for constant $c_{\rm e}$ and $d_{\rm p}$ should be a straight line. Thus the fraction of the different resistances in slurry system on the global rate could be distinguished.

2.2 Thermodynamic consideration of the hydrogen-benzene-cyclohexane ternary system

In this paper, we have to deal with the problems of gas-liquid equilibria of H_2-C_6H_6, H_2-C_6H_{12} and H_2-C_6H_6-C_6H_{12} systems. The thermodynamic behaviors of hydrogen in solutions highly deviate from the ideal state because hydrogen is a quantum gas. Connolly[9] studied the gas-liquid equilibrium of H_2-C_6H_6 system at temperatures up to 533 K and the system pressures up to 15.0 MPa. Although there are a few reports on the equilibrium data of H_2-C_6H_{12} binary system and H_2-C_6H_6-C_6H_{12} ternary system[10,11], values in corresponding ranges of the present experimental temperature and pressure are extremely limited. Kruyer and Nobel[11] revealed that the hydrogen solubility in C_6H_6-C_6H_{12} mixture was a linear function of the composition of mixture, and the hydrogen solubility in the mixture was the arithmetic mean of hydrogen solubilities in benzene and cyclohexane, respectively. It was also noted that the difference among the solubilities of the hydrogen in benzene, cyclohexane and benzene-cyclohexane mixture was not too large, probably attributed to the similarity of the molecular structure of benzene and cyclohexane. In view of the above-mentioned facts, the H_2-C_6H_6-C_6H_{12} ternary system was treated as the H_2-C_6H_6 binary system in this paper with the phase equilibrium data directly cited from Connolly[9].

3 EXPERIMENTAL FACILITIES AND PROCEDURES

3.1 Preparation and activation of the slurry

The hydrogenation reaction was conducted in a 500 ml FYX-05A stainless-steel autoclave (The Forth Meter Factory of Dalian, China). Fig. 2 shows the reaction system utilized in the present study. A desired amount of $MlNi_5$ was weighed and charged into the autoclave which was purged with vacuum pump immediately afterwards for about 15 min. The preparation procedures of $MlNi_5$ are reported elsewhere[5], and its density was 8.943 g·cm^{-3}. Hydrogen (99.99% pure) was then supplied until the system pressure reached 5.0 MPa. The $MlNi_5$ powder was activated inside the autoclave at room temperature for overnight. After 3 or 4 times activation, the hydrogen storage capacity of $MlNi_5$ reaches 170 ml·g^{-1}(S.T.P.), and the mean particle size of the alloy is 16.34 μm. Under the protection of nitrogen gas, a certain amount of benzene (A.R.), considering of the lost during the following procedures, was introduced into the autoclave. After the autoclave was evacuated, the prepared slurry

was then activated again at room temperature and a system pressure of 5.0 MPa with a stirring speed of 1000 r·min^{-1} for 3 or 4 times.

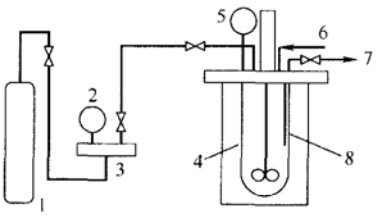

Figure 2 Schematic diagram of the experimental system

1—hydrogen source; 2,5—pressure gauge; 3—hydrogen reservoir; 4—stainless-steel autoclave; 6—liquid entrance; 7—vent-pipe; 8—thermocouple

3.2 Hydrogenation reaction of benzene

After complete activation of the slurry, the autoclave was evacuated again and heated to the designed reaction temperature, the hydrogen was then introduced to increase the pressure to a desired value. As the reaction proceeds, the pressure in the reactor was held constant over the entire experiment by adding the hydrogen continuously from the reservoir. The quantity of the consumed hydrogen in the autoclave was monitored by recording the reservoir pressure against time and could be used to calculate the hydrogen absorption capacity of the slurry as well as the reaction rate. The conversion of benzene in the liquid phase was analyzed by gas chromatogram.

4 RESULTS AND DISCUSSION

4.1 Typical hydrogen absorption behavior of $MlNi_5$-benzene slurry

Figure 3 shows the typical hydrogen absorption curve at a reaction temperature of 498 K and a system pressure of 5.0 MPa with an alloy concentration of 50% (by mass) (100 g $MlNi_5$+100 g C_6H_6), in which the conversion of benzene, one of the y-axis, was calculated from the hydrogen absorption which was valued from experimental record. This figure exhibits that the rate of reaction, given by the slope as (dc_e/dt), remained constant for the benzene conversion of more than 98%, indicating that the hydrogenation reaction of benzene in the slurry is zero order dependent on the concentration of benzene. At 498 K, after about 70 min reaction, benzene entirely converts into cyclohexane, and the saturated hydrogen absorption capacity of the slurry reaches 4.12% (by mass).

4.2 Influence of the alloy concentration on the reaction rate

Figure 4 shows the influence of the mass of $MlNi_5$ on the reaction rate. With the increasing of the concentration of $MlNi_5$, the hydrogenation reaction rate increases. According to Eq. (4), we plot $\frac{c_e}{r_{obs}}$ *vs.* $1/m$ in Fig. 5 which shows a good linear relationship between the two terms with the slope $\frac{\rho_p d_p}{6}\left(\frac{1}{k_c}+\frac{1}{k_s}\right)$ being 1.382×10^4 s·g·L^{-1}, and the intercept $\frac{1}{k_L a_g}$ being -6.48×10^{-4} s. The small value of $\frac{1}{k_L a_g}$ indicates that, for the slurry systems with high alloy concentrations of 15%—64%(by mass) in the present study, the mass transfer resistance at the gas-liquid interface can be neglected.

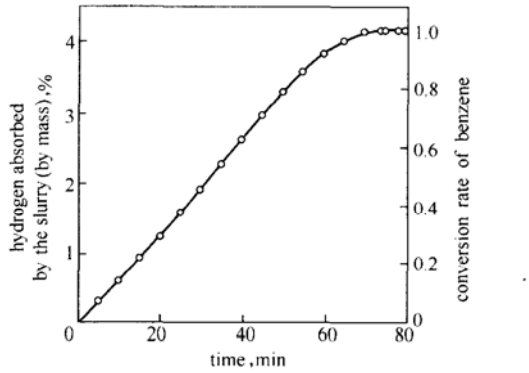

Figure 3 Typical hydrogen absorption behavior of slurry

(T: 498 K, p: 5.0 MPa, N: 1000 r·min^{-1}, slurry composition: 100 g C_6H_6+100 g $MlNi_5$)

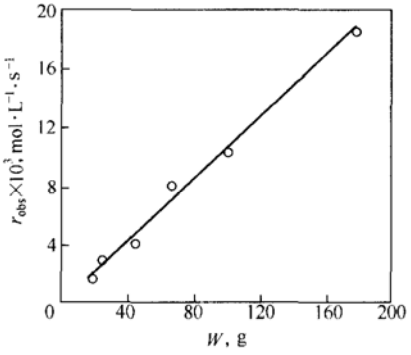

Figure 4 Influence of the weight of $MlNi_5$ on the reaction rate

(T: 498 K, p: 5.0 MPa, N: 1000 r·min^{-1}, 100 g C_6H_6 in the slurry)

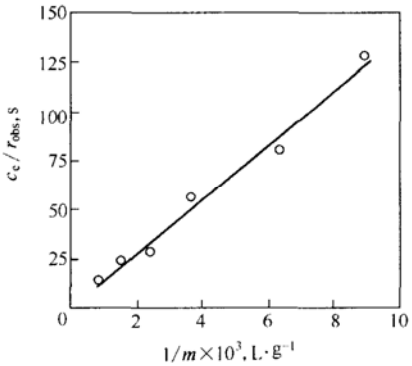

Figure 5 Relationship between c_e/r_{obs} and $1/m$

(T: 498 K, p: 5.0 MPa, N: 1000 r·min^{-1}, 100 g C_6H_6 in the slurry)

Table 1 Comparison of the mass transfer resistance and reaction resistance

T K	$D^a \times 10^4$ $cm^2 \cdot s^{-1}$	Pe^{*b}	Sh^c	$k_c^{*d} \times 10^3$ $m \cdot s^{-1}$	$k_c^e \times 10^3$ $m \cdot s^{-1}$	$1/k_c$ $s \cdot m^{-1}$	$\widetilde{V}^f$ $ml \cdot g^{-1}$	$r_{obs} \times 10^3$ $mol \cdot L^{-1} \cdot s^{-1}$	$x_{H_2}{}^g$	c_e $mol \cdot L^{-1}$	$1/k_s^h \times 10^{-6}$ $s \cdot m^{-1}$	$k_s \times 10^7$ $m \cdot s^{-1}$
393	2.357	3.731	2.629	3.79	7.58	131.8	1.299	0.90	0.0282	0.2783	9.7666	1.024
413	2.851	3.562	2.612	4.56	9.12	109.7	1.346	1.51	0.0282	0.2687	5.4291	1.842
433	3.521	3.409	2.596	5.59	11.2	89.38	1.396	2.11	0.0284	0.2607	3.6328	2.753
453	4.258	3.265	2.581	6.73	13.4	74.34	1.430	3.46	0.0285	0.2556	2.1211	4.714
473	5.269	3.137	2.568	8.28	16.6	60.39	1.488	5.12	0.0272	0.2345	1.2639	7.911
493	6.224	3.021	2.555	9.73	19.5	51.38	1.562	8.43	0.0282	0.2315	0.7217	13.86
513	7.555	2.916	2.544	11.8	23.6	42.52	1.656	10.54	0.0274	0.2123	0.4994	20.02

[a] Calculated according to Wilke and Chang's formula in Ref. [12], Page 515.

[b,c,d] Calculated according to Ref. [13], Chap.8.

[e] Usually, $k_c = 2k_c^*$, according to Ref. [13], Chap.8.

[f] Cited from Ref. [14], Chap.4.

[g] Cited from Connolly's experimental data[9].

[h] Calculated using Eq. (4).

4.3 Influence of temperature on the reaction rate

The hydrogen absorption rate of the slurry increases rapidly when the reaction temperature increases from 393 K to 513 K, and reaches the maximum value at 513 K (Fig. 6). If the temperature further increases, the reaction rate will sharply decrease and approach to zero at 553 K. In other experiments using the same slurry system, the dehydrogenation of cyclohexane was observed at the reaction temperature above 523 K. the reaction rate will sharply decrease and approach to zero at 553 K. In other experiments using the same slurry system, the dehydrogenation of cyclohexane was observed at the reaction temperature above 523 K. The decrease in reaction rate may be caused by the drop of the catalyst performance at high temperature, or the occurrence of dehydrogenation reaction. The exact explanation for these phenomena is not clearly known. Table 1 compares the mass transfer resistance of hydrogen from the bulk liquid to the particle surface ($1/k_c$) and the reaction resistance at the surface of the catalyst particles ($1/k_s$). The results revealed that $1/k_c$ can be neglected with the whole process controlled completely by the surface reaction. Thus the reaction rate equation can be simplified to

$$r_{obs} = k_s \cdot \frac{6m}{\rho_p d_p} \cdot c_e \qquad (5)$$

in which k_s, the constant of the surface reaction rate, may obey the Arrhenius equation

$$k_s = k_{s,0} \cdot e^{-Ea/RT} \qquad (6)$$

The plot of $\ln k_s$ *vs.* $1/T$ is shown in Fig. 7. The frequency factor $k_{s,0}$ and the activation energy Ea were obtained to be $3.76 \times 10^{-2}\ m \cdot s^{-1}$ and $42.16\ kJ \cdot mol^{-1}$, respectively. In the temperature range of 393—513 K, the apparent reaction rate of the liquid-phase hydrogenation of benzene in the slurry system is

$$r_{obs} = 3.76 \times 10^{-2} \cdot e^{-4.216 \times 10^4/RT} \cdot \frac{6m}{\rho_p d_p} \cdot c_e \qquad (7)$$

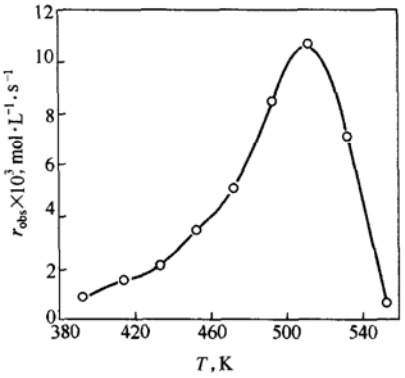

Figure 6 Influence of reaction temperature on the reaction rate
(p: 5.0 MPa, N: 1000 r·min^{-1}, slurry composition: 100 g C_6H_6+100 g $MlNi_5$)

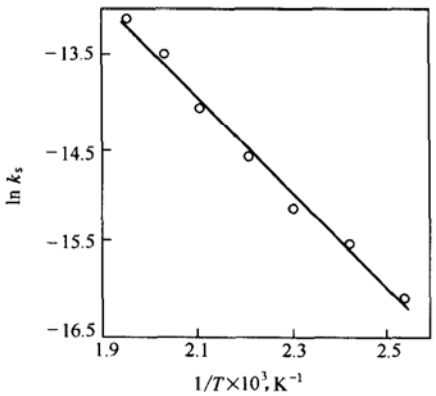

Figure 7 Relationship between $\ln k_s$ and $1/T$
(p: 5.0 MPa, N: 1000 r·min^{-1}, slurry composition: 100 g C_6H_6+100 g $MlNi_5$)

4.4 Influence of the liquid-phase hydrogen concentration on the reaction rate

With the increase in the system pressure, the specific volume of the liquid in the slurry decreases and

the hydrogen concentration in the liquid phase increases. Consequently, the hydrogenation reaction rate increases. The effect of the system pressure on the reaction rate was shown in Fig. 8.

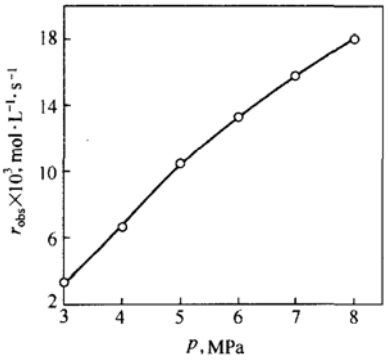

Figure 8 Influence of system pressure on the reaction rate
(T: 498 K, N: 1000 r·min^{-1}, slurry composition: 100 g C_6H_6+100 g $MlNi_5$)

To investigate the influence of the liquid-phase hydrogen concentration on the reaction rate, and to verify the kinetic model obtained above, it is assumed that the reaction rate is n-th order for the liquid-phase hydrogen concentration and can be written as

$$r_{obs} = k_s a_p \cdot c_e^n \tag{8}$$

Fig. 9 shows the relationship between $\ln r_{obs}$ and $\ln c_e$, which gives

$$r_{obs} = 0.038 \cdot c_e^{0.93} \tag{9}$$

$k_s a_p$ can also be calculated by the kinetic model obtained in Section 4.3. According to Eq. (7), at the temperature of 498 K $k_s a_p$ equals to 0.037, which is very consistent with the value in Eq. (9), 0.0038, obtained from the experimental data regression. Considering the experimental errors and the simplification in thermodynamic aspects, it is reasonable to conclude that the reaction rate is first order for liquid-phase hydrogen concentration.

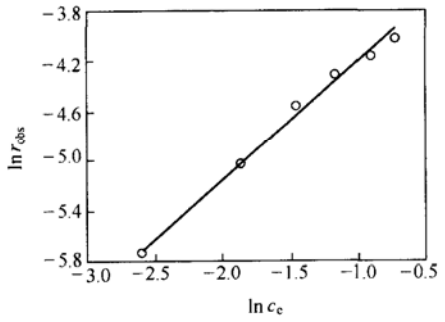

Figure 9 Relationship between $\ln r_{obs}$ and $\ln c_e$
(T: 498 K, N: 1000 r·min^{-1}, slurry composition: 100 g C_6H_6+100 g $MlNi_5$)

4.5 Effect of the stirring speed on the reaction rate

The reaction rate increases linearly with the increasing of the stirring speeds until 1250 r·min^{-1}. When the stirring speed exceeds 1250 r·min^{-1}, the reaction rate reaches a constant (Fig. 10). It indicates that the agitation power affects the bubble size in the slurry reactor, but its effects on the mass transfer coefficient at gas-liquid interface is not remarkable[13]. Moreover, besides keeping the solid particles suspending in the slurry, the vigorous stirring promotes the turbulence flow of the fluid enhancing the liquid-solid mass transfer. But for small particles, they tend to move with the liquid, the enhancement of the liquid-solid mass transfer coefficient is very limited. For $MlNi_5$-benzene systems in this work, the kinetic analyses reveal that the whole process is completely controlled by the surface reaction, and the mass transfer resistances at the gas-liquid and liquid-solid interfaces can be neglected. In this case, the main effect of the vigorous stirring is to keep the $MlNi_5$ particles suspending in the bulk liquid.

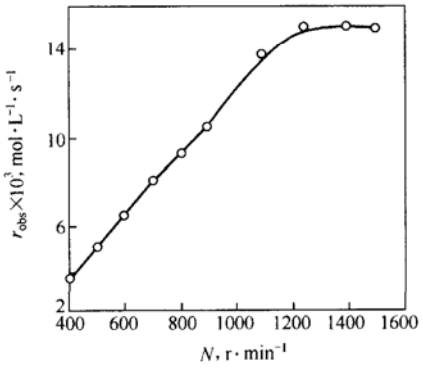

Figure 10 Effect of the stirring speed on the reaction rate
(T: 498 K, p: 5.0 MPa, slurry composition: 100 g C_6H_6+100 g $MlNi_5$)

Owing to the limitation of the designed working speed of the apparatus, the stirring speed is usually set at 1000 r·min^{-1} for ordinary operations in this work. It seems that this stirring speed does not produce an ideal suspending state of $MlNi_5$ particles in the slurry.

5 CONCLUSIONS

(1) The liquid-phase hydrogenation of benzene in $MlNi_5$-benzene slurry system is a surface reaction controlled process and the mass transfer resistances at the gas-liquid and liquid-solid interfaces can be confidently neglected.

(2) The apparent reaction order is zero for benzene and first order for hydrogen in liquid-phase. The variations of benzene or cyclohexane concentration in the slurry do not affect the reaction rate.

(3) In a temperature range of 393—513 K, the kinetic model of the liquid-phase hydrogenation of benzene in the $MlNi_5$-benzene slurry system can be written as

$$r_{obs} = 3.76 \times 10^{-2} \cdot e^{-4.216\times10^4/RT} \cdot \frac{6m}{\rho_p d_p} \cdot c_e$$

NOMENCLATURE

a_g	specific surface area of bubbles per unit liquid volume, m^{-1}
a_p	specific surface area of particles per unit liquid volume, m^{-1}
c_e	H_2 concentration on the liquid side at the gas-liquid surface, $mol \cdot L^{-1}$
c_l	H_2 concentration in the bulk liquid, $mol \cdot L^{-1}$
c_s	H_2 concentration in liquid phase contiguous to the surface of catalyst particles, $mol \cdot L^{-1}$
D	diffusivity of hydrogen in benzene, $cm^2 \cdot s^{-1}$
d_p	mean particle size, μm
k_c	liquid-solid mass transfer coefficient, $m \cdot s^{-1}$
k_c^*	liquid-solid mass transfer coefficient calculated by Pe^*, $m \cdot s^{-1}$
k_L	gas-liquid mass transfer coefficient, $m \cdot s^{-1}$
k_{obs}	first order apparent rate constant, $m \cdot s^{-1}$
k_s	constant of the surface reaction rate, $m \cdot s^{-1}$
$k_{s,0}$	frequency factor in Arrhenius Equation, $m \cdot s^{-1}$
m	load of catalyst per unit liquid volume ($m = W/V$), $g \cdot L^{-1}$
N	agitator speed, $r \cdot min^{-1}$
n	order of reaction
Pe^*	Peclet number free subsidence
p	pressure, MPa
r_{obs}	apparent reaction rate, $mol \cdot L^{-1} \cdot s^{-1}$
Sh	Sherwood number
T	reaction temperature, K
V	volume of the bulk liquid, L
$\widetilde{V}$	specific volume of benzene, $ml \cdot g^{-1}$
W	mass of the catalyst, g
x_{H_2}	molar fraction of hydrogen in liquid phase
ρ_p	density of $MlNi_5$, $g \cdot cm^{-3}$

REFERENCES

1 Reilly, J.J., Johnson, J.R., "The kinetics of the absorption of hydrogen by $LaNi_5H_x$-*n*-undecane suspensions", *J. Less-Common Met.*, **104**, 175—190 (1984).

2 Johnson, J.R., Reilly, J.J., "Kinetics of hydrogen absorption by metal hydride suspensions: The systems $LaNi_5H_x$/*n*-octane and $LaNi_{4.7}Al_{0.3}H_x$/*n*-undecane", *Z. Phys. Chem. Neue Folge*, **147**, 263—272 (1986).

3 Chen, C.P., Chen, L.X., Cai, G.M., An, Y., Xu, G.H., "Slurry materials for hydrogen absorption", CN 1380136A (2002).

4 Yasuaki Osumi, The Properties and Applications of Metal Hydride, Wu, Y.K., Miao, Y.Q., trans., Liu, Y., proofed, Chemical Industry Press, Beijing, 423 (1990). (in Chinese)

5 Cai, G.M., Chen, C.P., An, Y., Xu,G.H., Chen, L.X., Wang, Q.D., "Hydrogen absorption thermodynamic properties of rare earth based hydrogen storage alloy in benzene", *J. Rare Earths*, 20 (1), 28—30 (2002).

6 An, Y., Chen, C.P., Xu, G.H., Cai, G.M., Wang, Q.D., "A study on the kinetics of hydrogen absorption by metal hydride slurries. I. The absorption of hydrogen by hydrogen storage alloy $MlNi_5$ suspended in benzene", *J. Rare Earths*, **20** (2), 113—115 (2002).

7 An, Y., Chen, C.P., Xu, G.H., Cai, G.M., Wang, Q.D., "Study on kinetics of hydrogen absorption by metal hydride slurries. Ⅱ. Hydrogenation of benzene catalyzed by $MlNi_5$", *J. Rare Earths*, **20** (3), 231—233 (2002).

8 Smith, J.M., Chemical Engineering Kinetics, 3rd ed., McGraw-Hill, New York (1981).

9 Connolly, J.F., "Thermodynamic properties of hydrogen in benzene solutions", *J. Chem. Phys.*, **36**, 2897—2904 (1962).

10 Krichevskii, I.R., Sorina, G.A., "Phase and volume relations in liquid-gas systems under high pressure", *Zhur. Fiz. Khim.* (*Russian J. Phys. Chem.*), **32**, 2080—2086 (1958).

11 Kruyer, S., Nobel, A.P.P., "Solubility of hydrogen in benzene, cyclohexane, decalin, phenol and cyclohexanol", *J. Royal Netherlands Chem. Society*, **80**, 1145—1156 (1961).

12 Bird, R.B., Stewart, W.E., Lightfoot, E.N., Transport Phenomena, John Wiley & Sons, New York (1960).

13 Chen, G.T., Chemical Reaction Engineering, Chemical Industry Press, Beijing, 353—358 (1981). (in Chinese)

14 Hancock, E. G., Benzene and Its Industrial Derivatives, Ernest Benn Limited, London & Tonbridge, 120 (1975).